[47] P. J. M. Van Laarhoven, and E. H. L. Aarts, *Simulated Annealing: Theory and Applications*. Dordrecht, Holland: D. Reidel, 1987.
[48] T. Yokohira, M. Sugano, T. Nishida, and H. Miyahara, "Fault tolerant packet-switched network design and its sensitivity," *IEEE Trans. Rel.*, vol. 40, no. 4, pp. 452–460, 1991.

New Closed-Form Solution for Kinematic Parameter Identification of a Binocular Head Using Point Measurements

Sheng-Wen Shih, Yi-Ping Hung, and Wei-Song Lin

***Abstract*— This paper proposes a new closed-form solution for identifying the kinematic parameters of an active binocular head having four revolute joints and two prismatic joints by using three-dimensional (3-D) point (position) measurements of a calibration point. Since this binocular head is composed of off-the-shelf components, its kinematic parameters are unknown. Therefore, we can not directly apply those existing nonlinear optimization methods. Even if we want to use the nonlinear optimization methods, a closed-form solution can be first applied to obtain accurate enough initial values. Hence, this paper considers only methods that provide closed-form solutions, i.e., those requiring no initial estimates. Notice that most existing closed-form solutions require pose (i.e., both position and orientation) measurements. However, as far as we know, there is no inexpensive technique which can provide accurate pose measurements. Therefore, existing closed-form solutions based on pose measurements can not give us the required accuracy. As a result, we have developed a new method that does not require orientation measurements and can use only the position measurements of a calibration point to obtain highly accurate estimates of kinematic parameters using closed-form solutions. The proposed method is based on the complete and parametrically continuous (CPC) kinematic model, and can be applied to any kind of kinematic parameter identification problems with or without multiple end-effectors, providing that the links are rigid, the joints are either revolute or prismatic and no closed-loop kinematic chain is included. Simulations and real experiments have shown that the proposed method of using only point measurements is more robust against noise than those existing closed-form solutions using both position and orientation measurements when calibrating our binocular head.**

***Index Terms*— Active vision, binocular head, kinematic calibration, three-dimensional (3-D) circle fitting, 3-D line fitting.**

I. Introduction

A. Motivation

Many computer vision problems that are ill-posed, nonlinear, or unstable for a passive observer become well-posed, linear, or stable for an active observer [1]. Since it is able to acquire information actively, the active vision system has more potential applications than a passive one has. In an active stereo vision system, the cameras are able to perform functions such as gazing, panning, and tilting. To perform experiments on active vision, we have built a binocular head (referred to as the IIS head). The IIS head has four revolute joints and two prismatic joints, as shown in Fig. 1. The two joints on top of the IIS head are for camera vergence or gazing (referred to as joint $5L$ and joint $5R$). The next two joints below them are for tilting and panning the stereo cameras (referred to as joint 4 and joint 3). All of the above four joints are revolute, and are mounted on an X–Y table which is composed of two prismatic joints (referred to as joint 2 and joint 1). To control this head, we need to calibrate its kinematic model in advance. Because kinematic calibration is quite tedious, many researchers tend to avoid it. For example, Deriche *et al*. [2] have shown how to recover the epipolar geometry using an uncalibrated stereo rig. Krotkov [3] used a simplified model, namely the calibrated stereo disparity, and achieved the accuracy of about one part in 100 in estimating three-dimensional (3-D) depth. Our interest is to accurately control the stereo head for 3-D tracking and 3-D reconstruction. While the kinematic model is not an indispensable requirement, it can definitely simplify our task if we have a good estimate of the kinematic parameters.

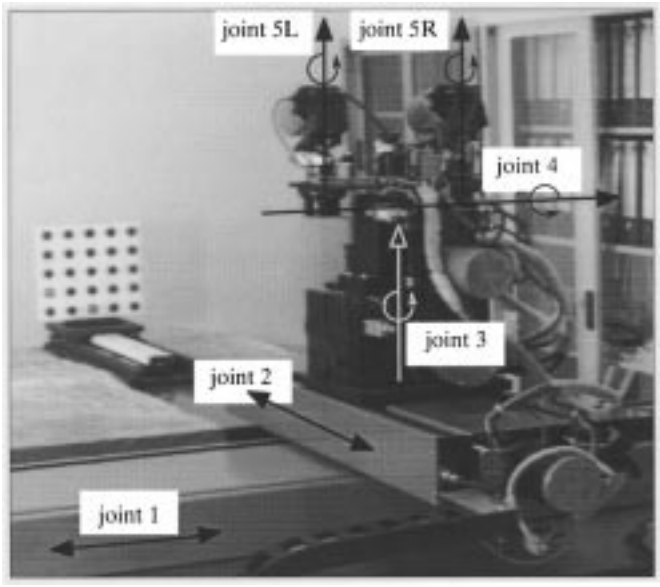

Fig. 1. A picture of the IIS head.

B. Why Closed-Form Solutions?

In this paper, our goal is to calibrate the kinematic parameters of the IIS head for controlling the orientations and positions of the stereo cameras. Since the IIS head was built with off-the-shelf components, its kinematic parameters are unknown. Therefore, we cannot directly apply those existing nonlinear optimization methods, e.g., [4]–[14], which all require good initial values. Even if we want to use the nonlinear optimization methods, a closed-form solution can be first applied to obtain accurate enough initial values. Theoretically, when using a nonlinear optimization technique, the initial values of the kinematic parameters must be as accurate as possible in order to obtain reliable calibration results.

C. Kinematic Calibration and Head/Eye Calibration

Two approaches have been considered in calibrating the binocular head: an integrated approach and a two-stage approach. The inte-

Manuscript received September 22, 1995; revised November 10, 1996. This work was supported in part by the National Science Council, Taiwan, under Grants NSC 83-0408-E-001-004, NSC 84-2213-E-001-011, and NSC 85-2213-E-001-016.

S.-W. Shih is with the Department of Computer Science and Information Engineering, National Chi Nan University, Puli Nantou 545, Taiwan, R.O.C. (e-mail: swshih@ncnu.edu.tw).
Y.-P. Hung is with the Institute of Information Science, Academia Sinica, Taipei 115, Taiwan, R.O.C. (e-mail: hung@iis.sinica.edu.tw).
W.-S. Lin is with the Department of Electrical Engineering, National Taiwan University, Taipei 106, Taiwan, R.O.C.

Publisher Item Identifier S 1083-4419(98)02195-5.

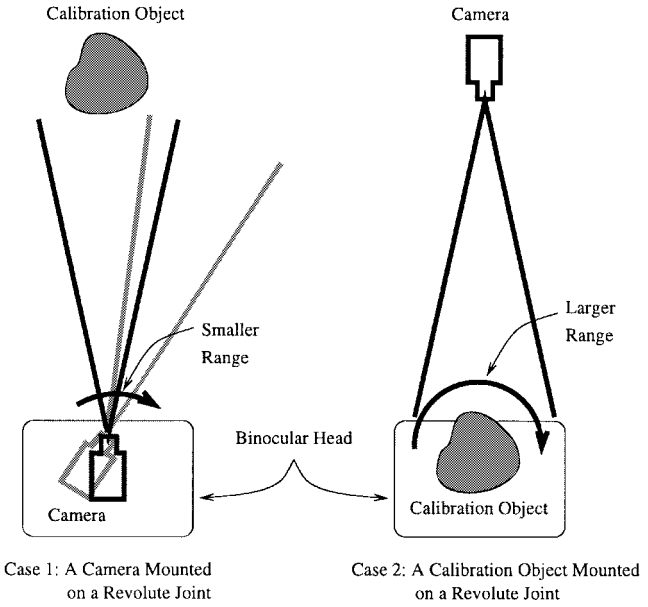

Fig. 2. By mounting a calibration object to the end-effector of a robot, the calibration range becomes much larger when using a visual sensor.

grated approach combines the kinematic calibration problem together with the head/eye calibration problem. Methods proposed by Zhuang and Roth [15], Shih *et al*. [16], and Young *et al*. [17] can be used to solve this combined problem. However, we encountered the following two major problems when using the existing methods to calibrate our IIS head. The first problem is that it is necessary to determine the poses of the cameras on the binocular head with respect to a calibration object. With our experience, the pose estimation techniques available in the literatures are not good enough to yield highly accurate estimates of the camera poses, especially when the distance between the camera and the calibration object is large, e.g., larger than 1 m. The second problem is that it is difficult to keep the calibration object in the field of view while rotating the cameras. Even if we can keep the calibration object in the field of view while rotating the cameras, it will restrict the motion range in the calibration (see Fig. 2). Hence, after the calibration, the binocular head would have large probability of working outside the small calibration range, which may lead to larger kinematic inaccuracy in general. For a Cartesian robot with eye-on-hand configuration [18], there is no such problem of keeping calibration object within the field of view because the offset caused by the revolute motion can be compensated by prismatic motion. However, since there is no vertical translation joint in our IIS head, there is no way to compensate the tilt axis rotation to keep the calibration object in the field of view. In addition to the aforementioned two problems, we may occasionally need to change the zoom and focus setting of the lens which would result in a new camera coordinate system. With the integrated approach, the tedious procedure for calibrating the head kinematics is needed for obtaining the new head/eye relation. To avoid the above problems, we chose a two-stage approach described below for calibrating our binocular head.

The two-stage approach solves the kinematic calibration problem and the head/eye calibration problem in two different stages. In the first stage, the two cameras on the IIS head are replaced by two small end-effector calibration plates having nine circles (see Fig. 3). The positions of the calibration plates, or equivalently, of the end-effectors, can be estimated using the stereo vision measurement system or other more accurate 3-D measurement systems, such as theodolite and coordinate measuring machines (CMM's) [19].

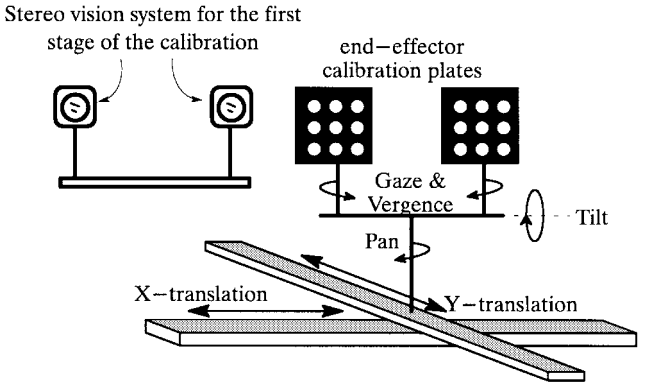

Fig. 3. The schematic diagram of the setup for the first stage of the calibration process.

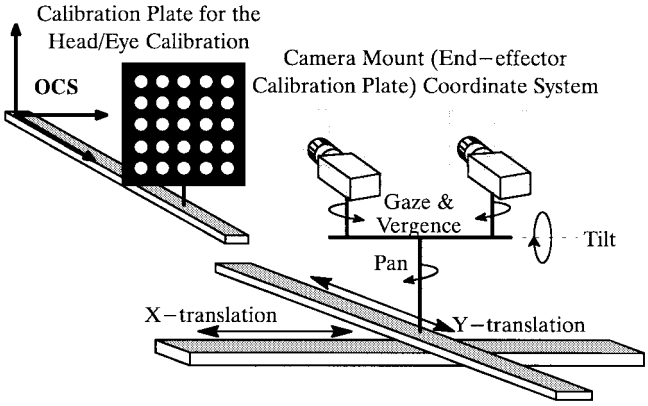

Fig. 4. The schematic diagram of the setup for the second stage of the calibration process.

Since the stereo vision measurement system is set apart from the binocular head and looks back to the calibration plates mounted on the head (as shown in Fig. 3), it is much easier to keep the calibration plates in the field of view while moving the joints of the head. The acquired positions of the calibration plates are then used to calibrate the kinematic parameters. In the second stage, the cameras are mounted back to the IIS head as show in Fig. 4. We can then use either of the methods proposed by Tsai and Lenz [20] or Shih *et al*. [21] to calibrate the head/eye relation. After the two-stage calibration, the robot kinematic and the head/eye relation are combined to provide a complete kinematic model for motion control. This paper will focus on the first stage of the calibration, i.e., the head calibration. However, the method can also be applied to the kinematic calibration of general robots.

D. Existing Closed-Form Solutions Using Pose Measurements

Most existing techniques that provide closed-form solutions estimate the joint axis from the pose measurements (i.e., orientation and position) of the end-effector, e.g., Lenz and Tsai [18] and Young *et al*. [17]. Recently, Zhuang and Roth [15], [22] and Shih *et al*. [16] have developed direct solutions to the CPC kinematic parameters [14], also by using the pose measurements of the end-effector. Notice that all the existing closed-form solutions estimate the orientation of the joint axis by finding the rotation axis of the relative orientation matrices obtained from the pose measurements. While the translation part of the kinematic parameters are either estimated joint by joint separately [16], [17] or solved all at one time [15], [22]. Methods proposed in [15] and [22] that solve all the translation

parameters at one time can reduce the translation error to some extent, but the solution is more complicated than those solving translation parameters joint by joint. Despite of the different kinematic models and different formulations, existing closed-form solutions based on pose measurements are essentially similar to each other and their accuracies are approximately of the same order. One problem of the existing closed-form solutions based on pose measurements is that they do not make the full use of all the information contained in the measurements. Instead, they use only the orientation information of the pose measurements when estimating the orientation of the joint axes. Hence, the orientation error of the estimated kinematic model would be of the same order of the orientation measurement error. This implies that one should not expect accurate kinematic calibration results when using the existing closed-form solutions based on pose measurements, unless accurate orientation measurements are available. Unfortunately, obtaining accurate measurement of a robot's orientation is known to be a difficult problem.

E. Existing Methods Using Only Point Measurements

The method presented in this paper requires no orientation measurements. The main idea is that the error-prone orientation estimation should be avoided, unless either a highly accurate CMM is available (not in normal vision laboratory setup, including ours), or a great amount of measurements are available to gain the robustness of the estimation (available in our setup). Our method is similar to that proposed by Stone [23] and Sklar [24]. With their approaches, the position and orientation of the joint axis are estimated from the measurements of the 3-D coordinates of a calibration point attached to the robot arm. When moving a revolute joint, the trajectory of the calibration point forms a 3-D circle. First, a plane is fitted to the measured calibration points by least-square technique. The resulted plane normal defines the orientation of the revolute joint axis. The measured calibration points are then projected along the plane normal onto the plane. A two-dimensional (2-D) circle is then fitted using nonlinear optimization method (which is achieved by iteratively applying a linear regression method), to find its center which defines the location of the joint axis. Notice that, in this approach, the orientation and location of the joint axis are separately estimated without using the information contained in the amount of rotation angles.

F. Organization of This Paper

In this paper, we propose a new closed-form solution based on the CPC kinematic model using 3-D point measurements of a calibration point. The advantages of using the CPC kinematic model are described in [14] and [15]. We shall show that by incorporating the information contained in the amount of rotation angles, a closed-form solution to the 3-D circle fitting problem can be derived. This paper is organized as follows. The kinematic calibration problem is formulated in Section II. The new closed-form solution is described in Section III. Experimental results are shown in Section IV. Conclusions are given in Section V.

II. Problem Formulation

Different coordinate systems associated with different joints of the IIS head are shown in Fig. 5. The coordinate frames $6L$ and $6R$ are the end-effector coordinate systems. The relation between any two consecutive joint frames can be characterized by a kinematic model. Consider Figs. 6 and 7. The CPC kinematic model we use for a revolute or prismatic joint is summarized below (see [14] and [25] for more details)

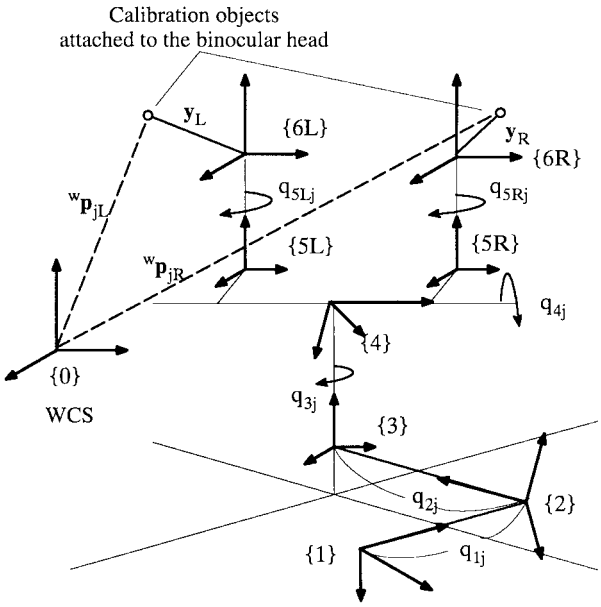

Fig. 5. The skeleton diagram of the IIS head.

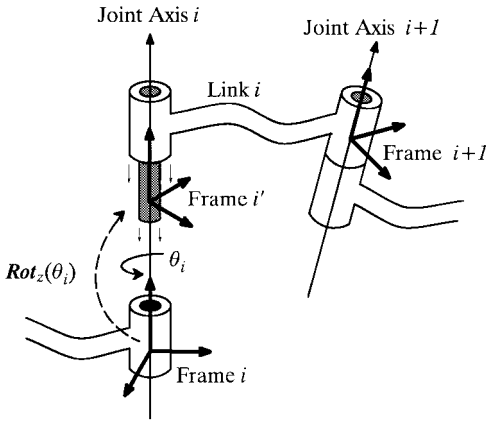

Fig. 6. CPC modeling convention for a revolute joint.

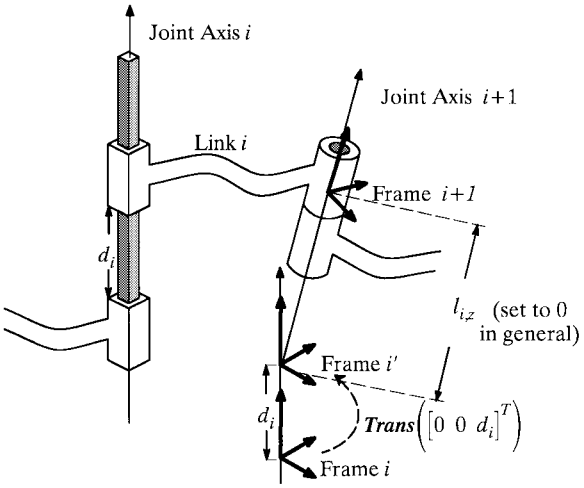

Fig. 7. CPC modeling convention for a prismatic joint.

$$ {}^{i}\boldsymbol{T}_{i+1} = {}^{i}\boldsymbol{T}_{i'}\,{}^{i'}\boldsymbol{T}_{i+1} \tag{1} $$

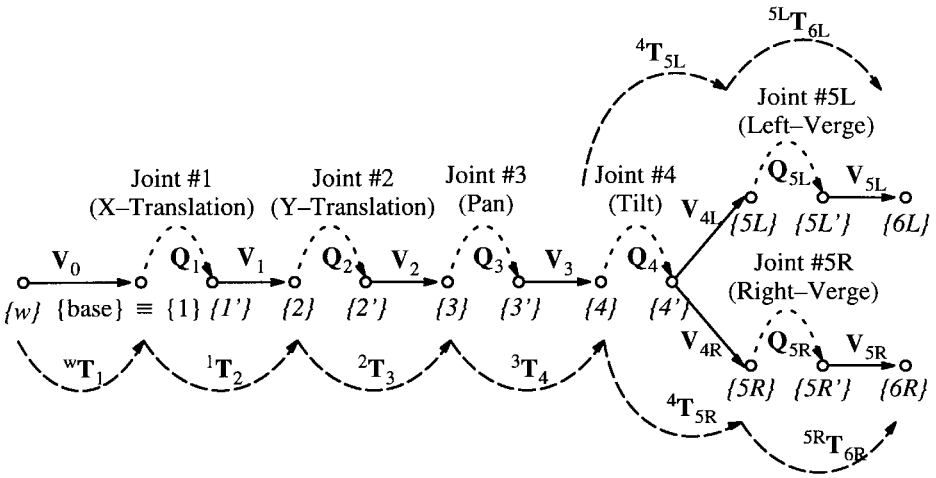

Fig. 8. Kinematic reference frames of the IIS head.

where

$$ {}^{i}\boldsymbol{T}_{i'} = \boldsymbol{Q}_i \tag{2} $$

$$ {}^{i}\boldsymbol{T}_{i+1} = \boldsymbol{V}_i \tag{3} $$

$$ \boldsymbol{Q}_i = \begin{cases} \mathbf{Rot}_z(q_i), & \text{for revolute joint,} \\ \mathbf{Trans}([0\ 0\ q_i]^t), & \text{for prismatic joint,} \end{cases} \tag{4} $$

$$ \mathbf{Rot}_z(\theta) = \begin{bmatrix} \cos(\theta) & -\sin(\theta) & 0 & 0 \\ \sin(\theta) & \sin(\theta) & 0 & 0 \\ 0 & 0 & 1 & 0 \\ 0 & 0 & 0 & 1 \end{bmatrix} \tag{5} $$

$$ \mathbf{Trans}([x\ y\ z]^t) = \begin{bmatrix} 1 & 0 & 0 & x \\ 0 & 1 & 0 & y \\ 0 & 0 & 1 & z \\ 0 & 0 & 0 & 1 \end{bmatrix} \tag{6} $$

$$ q_i = s_i q_i', s_i \in \{+1, -1\} \tag{7} $$

q_i' is the ith joint value

$$ \boldsymbol{V}_i = \boldsymbol{R}_i\ \mathbf{Rot}_z(\beta_i)\ \mathbf{Trans}([l_{i,x} l_{i,y} l_{i,z}]^t) \tag{8} $$

$$ \boldsymbol{R}_i = \begin{bmatrix} 1 - \dfrac{b_{i,x}^2}{1+b_{i,z}} & \dfrac{-b_{i,x}b_{i,y}}{1+b_{i,z}} & b_{i,x} & 0 \\ \dfrac{-b_{i,x}b_{i,y}}{1+b_{i,z}} & 1 - \dfrac{b_{i,y}^2}{1+b_{i,z}} & b_{i,y} & 0 \\ -b_{i,x} & -b_{i,y} & b_{i,z} & 0 \\ 0 & 0 & 0 & 1 \end{bmatrix} \tag{9} $$

$[b_{i,x}\ b_{i,y}\ b_{i,z}]^t$ is the unit orientation vector of the $(i+1)$st joint axis with respect to frame $\{i\}$ and $l_{i,x}, l_{i,y}$, and $l_{i,z}$ are the x-, y-, and z-components of the translation vector between two consecutive joint frames, respectively.

Note that the parameters, $\{\beta_i, l_{i,x}, l_{i,y}, l_{i,z}\}$, and $\{\beta_i, l_{i,z}\}$, are redundant for a prismatic and a revolute joint [14], respectively. Also, notice that for convenience we have introduced an intermediate coordinate system between the ith and $(i+1)$st frames, i.e., frame $\{i'\}$ in (8). From frame $\{i\}$ to frame $\{i'\}$, it is either a rotational or a translational motion matrix depending on the joint type, and from frame $\{i'\}$ to frame $\{i+1\}$, it is a fixed link matrix (referred to as a "shape" matrix in [14]) as defined in (8). By using the CPC kinematic model, the forward kinematic equation of the IIS head can be represented as follows (see Fig. 8):

$$ \begin{Bmatrix} {}^{w}\boldsymbol{T}_{6L}(q_j) \\ {}^{w}\boldsymbol{T}_{6R}(q_J) \end{Bmatrix} = {}^{w}\boldsymbol{T}_1\ {}^{1}\boldsymbol{T}_2(q_j)\ {}^{2}\boldsymbol{T}_3(q_j)\ {}^{3}\boldsymbol{T}_4(q_j) \cdot \begin{Bmatrix} {}^{4}\boldsymbol{T}_{5L}(q_j)\ {}^{5L}\boldsymbol{T}_{6L}(q_j) \\ {}^{4}\boldsymbol{T}_{5R}(q_j)\ {}^{5R}\boldsymbol{T}_{6R}(q_j) \end{Bmatrix} \tag{10} $$

where $q_j = [q_{1j}\ q_{2j}\ q_{3j}\ q_{4j}\ q_{5Rj}\ q_{5Lj}]$ denotes the joint values for the jth robot configuration, ${}^{i}\boldsymbol{T}_k$ denotes the transformation matrix from frame $\{i\}$ to frame $\{k\}$. For convenience, each of the transformation matrix is written as a function of the joint value vector, q_j, instead of q_{ij}.

Let y_L and y_R be the fixed coordinates of the calibration points mounted on the left and right end-effectors with respect to the left end-effector coordinate system (LECS) and right end-effector coordinate system (RECS), respectively. Let ${}^{w}p_{jL}$ and ${}^{w}p_{jR}$ denote the coordinates of the calibration points mounted on the left and right end-effectors, corresponding to the jth robot configuration, q_j, measured in the WCS. Transforming the coordinates of the calibration points, y_L and y_R, from LECS and RECS to the WCS, we have

$$ {}^{w}\tilde{p}_{jL} = {}^{w}\boldsymbol{T}_{6L}(q_j)\tilde{y}_L \tag{11} $$

and

$$ {}^{w}\tilde{p}_{jR} = {}^{w}\boldsymbol{T}_{6R}(q_j)\tilde{y}_R \tag{12} $$

where ${}^{w}\tilde{p}_{jL}$, ${}^{w}\tilde{p}_{jR}, \tilde{y}_L$, and $\tilde{y}_R$ are the 3-D homogeneous coordinates of ${}^{w}p_{jL}$, ${}^{w}p_{jR}, y_L$, and y_R, respectively.

With our new method, each joint is calibrated from the base toward the end-effectors. Without loss of generality, we assume that the kinematic parameters of the joints from the base to the ith joint have been known when calibrating the ith link matrix, i.e., $\boldsymbol{V}_i$. Only those joints with known kinematic parameters plus the $(i+1)$st joint are permitted to be moved. For example, when calibrating $\boldsymbol{V}_{4L}$, joints 1, 2, 3, 4 and $5L$ are allowed to be moved. From (10)–(12), we have

$$ {}^{i'}\tilde{p}_{jL} = {}^{i'}\boldsymbol{T}_{i+1}\ {}^{i+1}\boldsymbol{T}_{(i+1)'}\ {}^{(i+1)'}\tilde{y}_L \tag{13} $$

and/or

$$ {}^{i'}\tilde{p}_{jR} = {}^{i'}\boldsymbol{T}_{i+1}\ {}^{i+1}\boldsymbol{T}_{(i+1)'}\ {}^{(i+1)'}\tilde{y}_R \tag{14} $$

where

$$ {}^{i'}\boldsymbol{T}_{i+1} = \boldsymbol{V}_i \tag{15} $$

$$ {}^{i+1}\boldsymbol{T}_{(i+1)'} = \boldsymbol{Q}_{i+1} \tag{16} $$

$$ {}^{i'}\tilde{p}_{jL} = {}^{w}\boldsymbol{T}_{i'}(q_j)^{-1}\ {}^{w}\tilde{p}_{jL} \tag{17} $$

$$ {}^{i'}\tilde{p}_{jR} = {}^{w}\boldsymbol{T}_{i'}(q_j)^{-1}\ {}^{w}\tilde{p}_{jR} \tag{18} $$

$$ {}^{(i+1)'}\tilde{y}_L = {}^{(i+1)'}\boldsymbol{T}_{6L}(q_j)\ \tilde{y}_L \tag{19} $$

and

$$ {}^{(i+1)'}\tilde{y}_R = {}^{(i+1)'}\boldsymbol{T}_{6R}(q_j)\ \tilde{y}_R. \tag{20} $$

Note that if the ith link is a common links, i.e., a link between the world reference frame and joint 4, then both of the above two equations are valid (see Fig. 5); otherwise, only one of the (13) and (14) is valid.

From (13) and (14), we have

$$\boldsymbol{V}_i^{-1}\,{}^{i'}\tilde{p}_{jL} = \boldsymbol{Q}_{i+1}\,{}^{(i+1)'}\tilde{y}_L \tag{21}$$

and/or

$$\boldsymbol{V}_i^{-1}\,{}^{i'}\tilde{p}_{jR} = \boldsymbol{Q}_{i+1}\,{}^{(i+1)'}\tilde{y}_R. \tag{22}$$

Note that in our method, a robot kinematic calibration problem is divided into a sequence of subproblems of calibrating single revolute or prismatic joint. When calibrating a single joint, in addition to estimating unknown kinematic parameters, we also have to estimate the unknown 3-D position of a calibration point, i.e., $\tilde{y}_L$ and $\tilde{y}_R$ in (21) and (22), respectively. Therefore, the calibration point can be mounted at different positions when calibrating different joints. If link i is shared by both the left and right kinematic chains, we can simply use either of the two calibration (21) and (22). However, because taking the average of (21) and (22) can reduce some effects of measurement noise, we chose to use the average of (21) and (22). This is equivalent to using a pseudocalibration point in the middle of the left and right calibration point. Hence, we have (23)–(26), as shown at the bottom of the page.

Then, (21)–(23) can be unified as follows:

$$\boldsymbol{V}_i^{-1}\,{}^{i'}\tilde{p}_j = \boldsymbol{Q}_{i+1}\,{}^{(i+1)'}\tilde{y}. \tag{27}$$

Note that (27) is actually formulating the 3-D circle and 3-D line fitting problems for a revolute and prismatic joints (see Figs. 9 and 10), respectively. The unknown parameters to be estimated are the link matrix, $\boldsymbol{V}_i$, and the vector, ${}^{(i+1)'}y$. For the case of IIS head, our goal is to estimate the kinematic parameters: $\boldsymbol{V}_0, \boldsymbol{V}_1, \boldsymbol{V}_2, \boldsymbol{V}_3, \boldsymbol{V}_{4L}$, and $\boldsymbol{V}_{4R}$, using (27). In this case, we can set $\boldsymbol{V}_{5L} = I$ and $\boldsymbol{V}_{5R} = I$, because no matter what values $\boldsymbol{V}_{5L}$ and $\boldsymbol{V}_{5R}$ assumed in this stage, we always have to estimate a new head/eye relations, i.e., new $\boldsymbol{V}_{5L}$ and $\boldsymbol{V}_{5R}$, when cameras are mounted to the IIS head.

III. New Method for Kinematic Parameters Identification

Using (27), our new method will calibrate the ith link matrix by moving the $(i+1)$st joint (joints 1, 2, $\cdots, i$ can be moved too). For convenience, let R_{V_i}, R_i, and $Rot_z(\theta)$ be the 3×3 rotation matrix of $\boldsymbol{V}_i, \boldsymbol{R}_i$ and $\mathbf{Rot}_z(\theta)$, respectively. Let t_{V_i} be the 3×1 translation vector of matrix $\boldsymbol{V}_i$, and l_i denote the 3-D vector $[l_{i,x}\ l_{i,y}\ l_{i,z}]^t$. Using (8), we have

$$R_{V_i} = R_i Rot_z(\beta_i) \tag{28}$$

$$t_{V_i} = R_{V_i} l_i \tag{29}$$

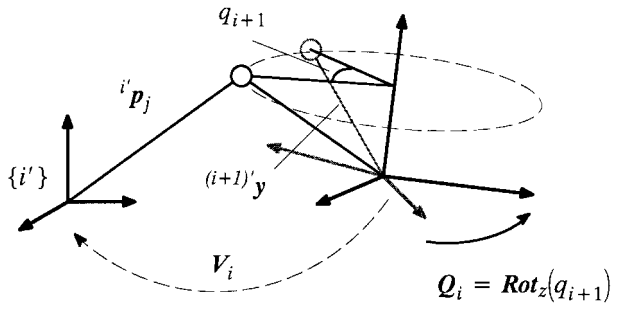

Fig. 9. Equation (27) is equivalent to a 3-D circle fitting problem for a revolute joint.

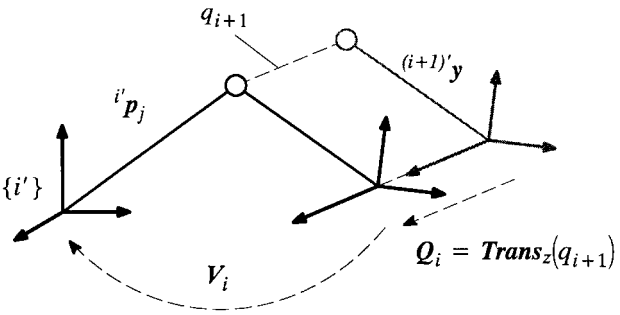

Fig. 10. Equation (27) is equivalent to a 3-D line fitting problem for a prismatic joint.

and

$$\boldsymbol{V}_i = \boldsymbol{R}_{V_i}\ \mathbf{Trans}(l_i) \tag{30}$$

which will be used in the following derivation.

A. Kinematic Parameter Identification for a Prismatic Joint

The redundant parameters and the unknowns for a prismatic joint are listed as follows for clarity of our derivation:

1) four given redundant parameters (typically set to zero if not prespecified for specific reason): β_i and l_i;
2) the unknowns: $R_i, {}^{(i+1)'}\tilde{y}$ and the sign parameter, s_i.

Consider (27). For a prismatic joint, we have

$$\boldsymbol{V}_i^{-1}\,{}^{i'}\tilde{p}_j = \mathbf{Trans}([0\ 0\ q_{(i+1)j}]^t)\,{}^{(i+1)'}\tilde{y} \tag{31}$$

or, using (30)

$$R_{V_i}^t\,{}^{i'}p_j - l_j = {}^{(i+1)'}y + [0\ 0\ q_{(i+1)j}]^t. \tag{32}$$

$$\boldsymbol{V}_i^{-1}\,{}^{i'}\tilde{p}_{jLR} = \boldsymbol{Q}_{i+1}\,{}^{(i+1)'}\tilde{y}_{LR} \tag{23}$$

where

$${}^{i'}\tilde{p}_{jLR} = \frac{({}^{i'}\tilde{p}_{jL} + {}^{i'}\tilde{p}_{jR})}{2} \tag{24}$$

and

$${}^{(i+1)'}\tilde{y}_{LR} = \frac{({}^{(i+1)'}\tilde{y}_L + {}^{(i+1)'}\tilde{y}_R)}{2} \tag{25}$$

$$\text{Here, we let} \begin{cases} {}^{i'}\tilde{p}_j = {}^{i'}\tilde{p}_{jLR}, {}^{i+1)'}\tilde{y} = {}^{(i+1)'}\tilde{y}_{LR} & \text{if link } i \text{ is shared by the left and right kinematic chains} \\ {}^{i'}\tilde{p}_j = {}^{i'}\tilde{p}_{jL}, {}^{(i+1)'}\tilde{y} = {}^{(i+1)'}\tilde{y}_L, & \text{if link } i \text{ belongs to the left branch only} \\ {}^{i'}\tilde{p}_j = {}^{i'}\tilde{p}_{jR}, {}^{(i+1)'}\tilde{y} = {}^{(i+1)'}\tilde{y}_R, & \text{if link } i \text{ belongs to the right branch only} \end{cases} \tag{26}$$

Notice that the value of ${}^{i'}p_j$ depend on the movements of joints $1, \cdots, i$ and can be computed using equations (17) and/or (18).

Multiplying R_{V_i} to both sides of (32) and noticing that

$$R_{V_i}\begin{bmatrix}0\\0\\q_{(i+1)j}\end{bmatrix} = R_i Rot_z(\beta_i)\begin{bmatrix}0\\0\\q_{(i+1)j}\end{bmatrix} = q_{(i+1)j}b_i \tag{33}$$

where $b_i = [b_{i,x}b_{i,y}b_{i,z}]^t$ is the third column vector of the rotation matrix R_i, we have

$${}^{i'}p_j = a + q_{(i+1)j}b_i \tag{34}$$

where $a = R_{V_i}(l_i + {}^{(i+1)'}y)$ is independent of configuration q_j. It is obvious that l_i is redundant, since l_i and ${}^{(i+1)'}y$ can not be independently estimated. Therefore, l_i can be set to zero if it is not prespecified for specific reason.

Suppose there are M measurements from M robot configurations, i.e., ${}^{i'}p_j$ and $q_{(i+1)j}, j = 1, 2, \cdots, M$. The kinematic parameter b_i can be estimated by minimizing the following error:

$$\epsilon = \sum_{j=1}^{M} \| {}^{i'}p_j - a - q_{(i+1)j}b_i \|^2 \tag{35}$$

subject to $b_i^t b_i = 1$.

The solution is (refer to [25] for the proof)

$$b_i = \frac{\sum_{j=1}^{M}(\Delta p_j \Delta q_{(i+1)j})}{\left\| \sum_{j=1}^{M}(\Delta p_j \Delta q_{(i+1)j}) \right\|} \tag{36}$$

where

$$\Delta p_j = {}^{i'}p_j - {}^{i'}\overline{p} \tag{37}$$

$$\Delta q_{(i+1)j} = q_{(i+1)j} - \overline{q}_{(i+1)} \tag{38}$$

$${}^{i'}\overline{p} = \frac{1}{M}\sum_{j=1}^{M} {}^{i'}p_j \tag{39}$$

and

$$\overline{q}_{(i+1)} = \frac{1}{M}\sum_{j=1}^{M} q_{(i+1)j}. \tag{40}$$

Notice that if the third component of b_i is negative, in order to be consistent with the CPC convention, we should change the sign of b_i and let $s_i = -1$; otherwise, let $s_i = +1$. Once the unit vector b_i is obtained, the rotation matrix, R_i, can be computed with (9). Finally, ${}^{(i+1)'}y$ can be solved by using (32). However, we do not have to calculate ${}^{(i+1)'}y$ if it is not of interest.

B. Kinematic Parameter Identification for a Revolute Joint

The redundant parameters and the unknowns for a revolute joint are listed below for clarity of the derivation:

1) two given redundant parameters (typically set to zero if not prespecified for specific reason): β_i and the z-component of l_i;
2) the unknowns: R_i, the sign parameter, s_i, ${}^{(i+1)'}y$, and the first two components of l_i.

For a revolute joint, the calibration equation can be derived from (27) that

$$R_{V_i}^t\, {}^{i'}p_j - l_i = Rot_z(q_{(i+1)j})\, {}^{(i+1)'}y \tag{41}$$

by using (30). For convenience, we decompose ${}^{(i+1)'}y$ into two portions as follows. Let ${}^{(i+1)'}y = [y_1\ y_2\ y_3]^t$, and

$${}^{(i+1)'}y = y_a + y_b \tag{42}$$

where $y_a = [y_1\ y_2\ 0]^t$ and $y_b = [0\ 0\ y_3]^t$. Note that for any y_1 and $y_2, y_1^2 + y_2^2 \neq 0$, there exists a scalar ρ and a rotation angle ω such that

$$y_a = \rho Rot_z(\omega)e_1 \tag{43}$$

where $e_1 = [1\ 0\ 0]^t, \rho = \sqrt{y_1^2 + y_2^2}, \omega$ is the angle between the vector y_a and the x-axis. Substituting equations (42) and (43) into (41), we have (by noting that $y_b = Rot_z(\cdot)y_b$)

$$Ru_j + t = \rho v_j \tag{44}$$

where $R = Rot_z(-\beta_i - \omega)R_i^t, u_j = {}^{i'}p_j, t = -Rot_z(-\omega)l_i - y_b$ and $v_j = Rot_z(q_{(i+1)j})e_1$. R, t and ρ can be solved by minimizing the following error using the least-square method:

$$e = \sum_{j=1}^{M} \| Ru_j + t - \rho v_j \|^2. \tag{45}$$

The procedures for calculating a closed-form solution to (45) are listed in the following (refer to [25] for more details).

Step 1: Compute $\overline{u} = (1/M)\Sigma_{j=1}^{M}\ u_j, \overline{v} = (1/M)\Sigma_{j=1}^{M}\ v_j, \underline{u}_j = u_j - \overline{u}$ and $\underline{v}_j = v_j - \overline{v}$.

Step 2: Let $A = [\underline{v}_1 \cdots \underline{v}_j \cdots \underline{v}_M]$ and $B = [\underline{u}_1 \cdots \underline{u}_j \cdots \underline{u}_M]$.

Step 3: Compute the 3×3 matrix $C = BA^t$.

Step 4: Compute the singular value decomposition

$$C = U\begin{bmatrix}s_1 & 0 & 0\\0 & s_2 & 0\\0 & 0 & s_3\end{bmatrix}V^t$$

where $s_1 \geq s_2 \geq s_3 \geq 0$.

Step 5: If $\det(VU^t) = +1$, then compute $\hat{R} = VU^t$, otherwise, let

$$\hat{R} = V\begin{bmatrix}1 & 0 & 0\\0 & 1 & 0\\0 & 0 & -1\end{bmatrix}U^t.$$

Step 6: Compute $\rho = [\Sigma_{j=1}^{M}\ \underline{u}^t R\underline{v}_j][\Sigma_{j=1}^{M}\ \underline{v}_j^t\underline{v}_j]^{-1}$.

Step 7: Compute $t = \rho\overline{v} - R\overline{u}$.

We now show how to compute the kinematic parameters, R_i and l_i, from R and t. Remember that $R = Rot_z(-\beta_i - \omega)R_i^t$, as defined following (44). It is obvious that the third rows of R and R_i^t, i.e., b_i^t, should be the same. Therefore, b_i^t can be obtained from the third row of the matrix R. Notice that if the third component of b_i is negative, in order to be consistent with the CPC convention, we should change the sign of b_i and let $s_i = -1$; otherwise, let $s_i = +1$. From (8) and (9), we can compute R_{V_i} from b_i and β_i. Then we can compute $Rot_z(\omega)$ using the following relation:

$$Rot_z(\omega) = R_{V_i}^t R^t. \tag{46}$$

Remember that $y_b = [0\ 0\ y_3]^t$ and $t = -Rot_z(-\omega)l_i - y_b$ as defined following (42) and (44), respectively, hence

$$l_i + y_b = -Rot_z(\omega)t \tag{47}$$

where the z-component of l_i is a given redundant parameter, and y_b should be determined to make the above three equations of three unknowns consistent.

IV. Experiments

To evaluate the accuracy of robot calibration in the experiments, we use both positioning and orientation errors defined below as the error measures. The *positioning error* is defined as the Euclidean distance between the measured and predicted positions of the end-effector, where the predicted position is obtained by using the identified kinematic parameters. The *orientation error* is defined as the angle between the true and predicted orientation of the last two joint axes, i.e., joint $5L$ and joint $5R$. Notice that, in the real experiments, because the true orientation of the last two joint axes are unknown, only the positioning error was evaluated.

For comparison, we have also implemented two kinematic calibration methods modified from the methods proposed by Zhuang [22] and by us [16], both of which use pose measurements. The major modification we have made here is to reverse the order of the kinematic parameter identification in the original methods such that the kinematic parameters are calibrated from the base toward the end-effector. Notice that this modification is important, because if we calibrate a multiple-end-effector robot from the end-effectors to the base, at the link having two branching kinematic chains, we need to estimate an additional transformation matrix for unifying the coordinate systems from different end-effectors, which would introduce additional estimation error. The results of our original pose method [16] were shown in [26], which is three times worse than the modified pose method implemented here. Nevertheless, the point method proposed in this paper is at least twice more accurate than the modified methods using pose measurements, as shown in Figs. 15–17. For convenience, the proposed point method will be referred to as *Method-I* and the pose methods modified from [22] and [16] will be referred to as *Method-II* and *Method-III*, respectively. Notice that, for *Method-II* and *Method-III*, the procedure for estimating orientation kinematic parameters are exactly the same; therefore, the orientation error of these two methods will be identical.

The 3-D measurement system we used was a stereo vision system consisted of two Panasonic GP-MF 502 CCD cameras with a baseline of 524 mm, where their focal lengths were approximately 15 mm and the dimension of the sensor cell was about 10 μm, which provided 3-D measurement accuracy of 0.4 mm in z-direction and 0.2 mm in both x- and y-directions if the object distance was approximately 1.5 m and the deviation of the 2-D observation error was 0.1 pixel. Each small calibration plate attached to the camera mount has nine white disks as shown in Fig. 11. As shown in Fig. 12, in this paper, the input measurement data for *Method-I*, *Method-II* and *Method-III* are extracted from the same set of raw measurements, i.e., the 3-D position measurements of the nine disks on the calibration plate. The pose measurements were obtained by using the following procedure:

1) use the stereo vision system to measure the 3-D coordinates of the nine disks on the calibration plate, $\tilde{c}_i, i = 1, 2, \cdots, 9$;
2) compute the optimal solution of the following error function by using the Arun *et al.* method [27]

$$\min_{\boldsymbol{T_m}} \sum_{i=1}^{9} \|\tilde{d}_i - \boldsymbol{T_m}\tilde{c}_i\| \tag{48}$$

where $\tilde{d}_i$ is the homogeneous 3-D coordinates of the nine disks on the calibration plate with respect to the calibration plate coordinate system (see Fig. 11).

Both the position and orientation measurements, i.e., $\boldsymbol{T_m}$, were fed to *Method-II* and *Method-III*, while only the position measurements, i.e., the translation vector of $\boldsymbol{T_m}$, were fed to *Method-I*. Computer simulations have been conducted for studying errors of both the position and orientation of the estimated pose of the end-effector calibration plates, i.e., $\boldsymbol{T_m}$. In this simulation, we assume the error source is mainly in the estimation of the 2-D image location of the nine disks on the calibration plate. Each data point shown in Figs. 13 and 14 are obtained from the root mean square error of 1000 random trials. The relation between the 2-D image measurement noise and the 3-D *position* measurement error of our system configuration is shown in Fig. 13, while the relation between the 2-D measurement noise and the *orientation* error of $\boldsymbol{T_m}$ is shown in Fig. 14. Because the 2-D image measurement noise in our stereo vision measurement system is approximately of 0.1 pixel, the induced 3-D orientation error of $\boldsymbol{T_m}$ is approximately 0.25° which is not good enough for the kinematic calibration. Although the orientation estimation error can be reduced by choosing a larger calibration object, it is difficult for us to increase the size of the calibration object due to the limitations both on the payload of the binocular head and on the effective view field of our stereo vision system.

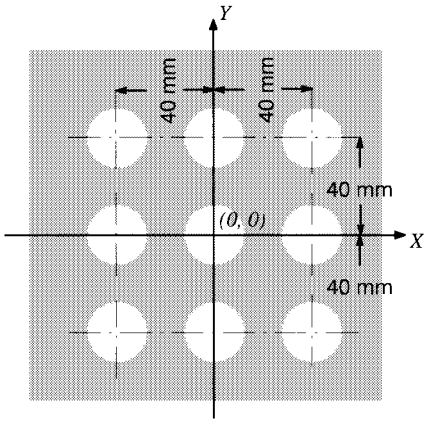

Fig. 11. The aspect of our end effector calibration plate and the calibration plate coordinate system defined on it.

In the first experiment (real experiment), twenty measurements were taken for each joint. Also, for testing the calibration accuracy we took extra 19 measurements with arbitrary configurations. We then chose M from the 20 measurements to calibrate the robot and used all of the 19 testing measurements to test the estimated parameters. The results are shown in Fig. 15 for $M = 4, 6, \cdots, 20$. One purpose of this experiment is to determine a proper number, M, such that the position error is less than 1 mm. Fig. 15 shows that *Method-I* can achieve higher accuracy than *Method-II* and *Method-III*. Notice that Fig. 15 does not show the potential that the position error decreases when M increases. We believe that it is because the nongeometric error dominates and the random noise induced error is relatively negligible. However, whatever M is, the error is less than 1 mm. As a result, we simply use $M = 20$ in the following experiments.

In the second experiment, computer simulations were conducted using the kinematic parameters obtained from the previous real experiment. Because the calibration plates were manufactured with very high accuracy—much higher than our 3-D stereo vision measurement accuracy, we assume that the 3-D stereo measurement noise is mainly due to the 2-D image observation error with a standard deviation of 0.1 pixels. Each data points shown in Fig. 16 is the average of 50 random trials. Fig. 16 also shows that *Method-I* can achieve higher accuracy than *Method-II* and *Method-III*. Notice that in the real experiments, the test data also contain measurement errors. Also, the joints of the IIS head are not ideal at all. Therefore, the real experimental results (in Fig. 15) have larger position error than the simulation ones (Fig. 16).

The last experiment is to test the robustness of the calibration algorithm. The 2-D observation error is assumed to be a normal random noise with zero mean and variance σ_{2D}. Fig. 17 shows the

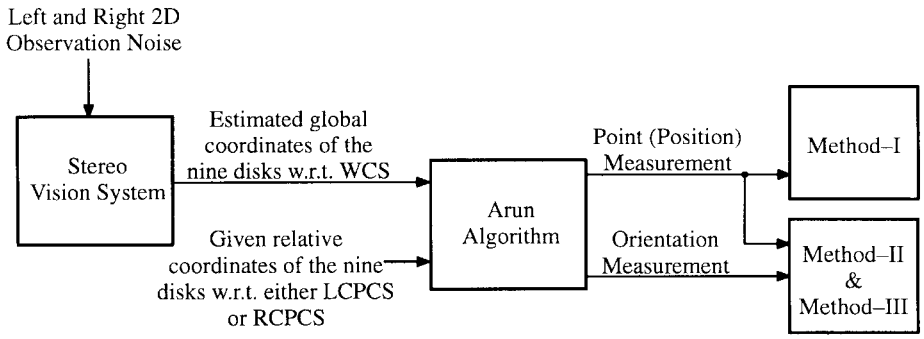

Fig. 12. The procedure for acquiring the pose (position and orientation) measurement of the calibration plate mounted on the end-effector for different methods tested in this paper.

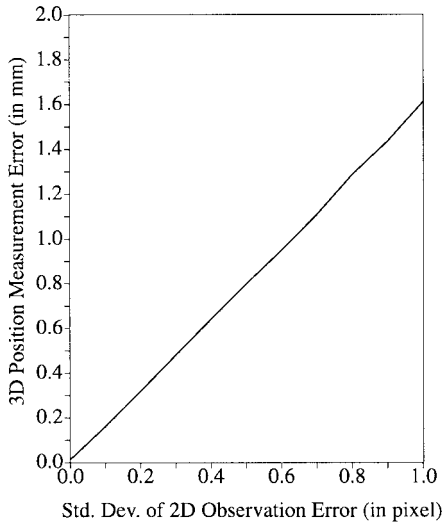

Fig. 13. The point measurement error of end effectors induced by the 2-D measurement noise.

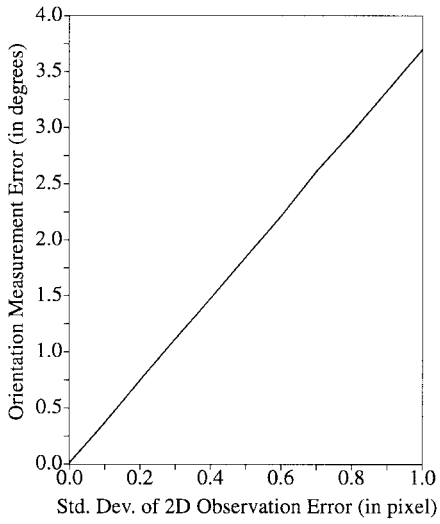

Fig. 14. The orientation measurement error of end effectors induced by the 2-D measurement noise.

results from computer simulations, where each point is obtained from the average of 50 random trials, for $\sigma_{2D} = 0.0$–1.0 pixel. The number of measurements for each joint is set to 20 as in the real experiment. The positioning error of this experiment shows that the proposed method is robust against the observation noise than the other two methods using pose measurements. However, these three methods have almost the same performance in estimating orientation parameters in this experiment.

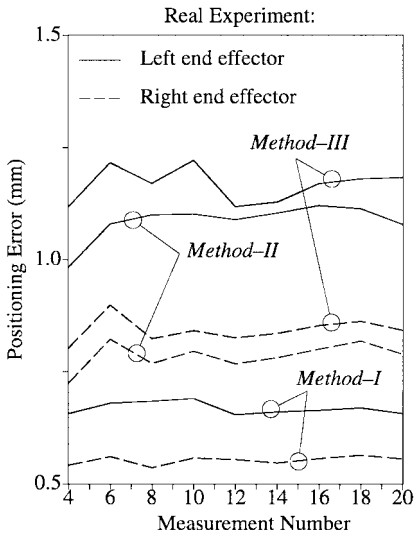

Fig. 15. The 3-D positioning error of two end effectors with respect to three calibration methods versus the measurement number (19 test points).

V. Conclusions

Active vision is attracting more and more research interest in the field of computer vision. Being able to acquire information actively, an active vision system has more potential applications than a passive one has. To control the positions and orientations of the cameras, the kinematic parameters of an active vision mechanism have to be known. Unfortunately, exact kinematic parameters are usually unknown. In this paper we have solved the kinematic parameter identification problem for the IIS head based on the CPC kinematic model. Four main features of our new method are described below.

1) With our new method, the kinematic parameters estimation problem is decomposed into many subproblems of single joint axis. Hence, the complexity is reduced and an easier implementation is derived. Also, this decomposition leads to a general solution for kinematic calibration of any robot with arbitrary combination of prismatic and revolute joints. Notice that this does not mean that only one joint can be moved at a time during the data collection phase. Instead, all the *calibrated* joints can be moved to gather more information.

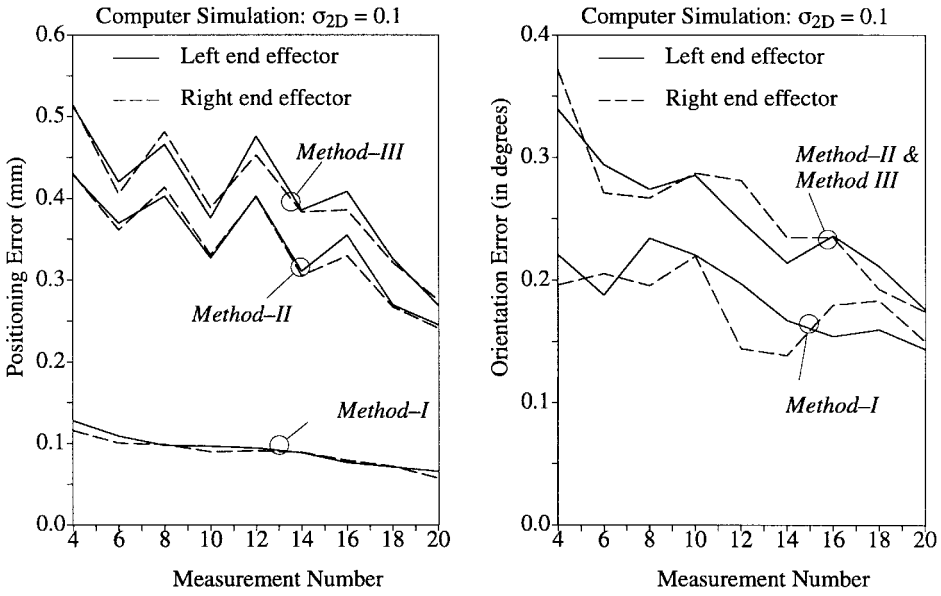

(a) (b)

Fig. 16. (a) The 3-D positioning error of the two end effectors with respect to three calibration methods versus the measurement number. (b) The orientation error of the left and right vergence axes with respect to three calibration methods versus the measurement number.

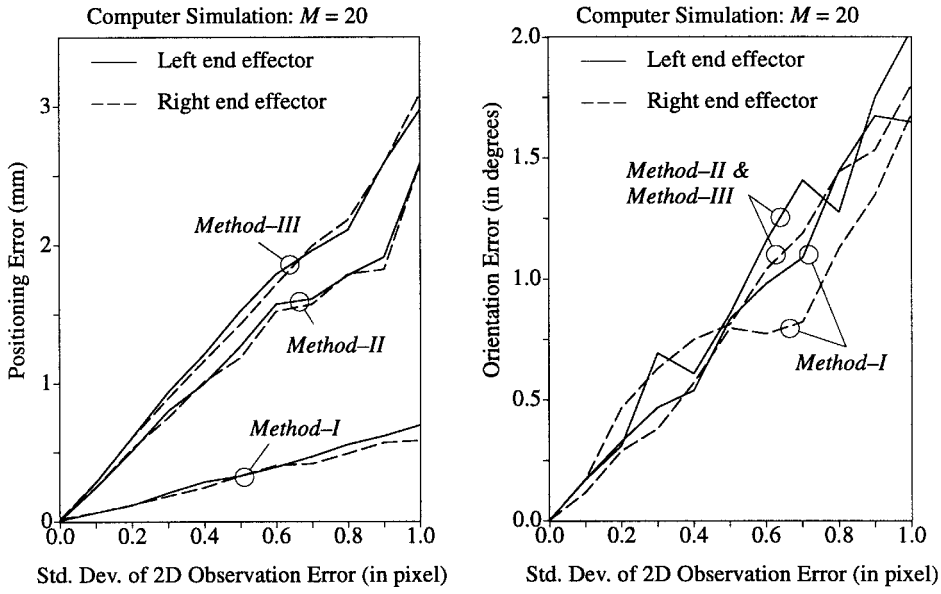

(a) (b)

Fig. 17. (a) The 3-D positioning error of the two end effectors with respect to three calibration methods versus the 2-D measurement noise. (b) The orientation error of the left and right vergence axes with respect to three calibration methods versus the 2-D measurement noise.

2) It is easier to obtain an accurate point measurement than to obtain an accurate pose measurement. Moreover, the calibration object can be of smaller size when using point measurements, which allows larger motion range of a joint in kinematic calibration and leads to more accurate and robust estimations of kinematic parameters.
3) With our method, each joint is calibrated in the order of from the base to the end-effectors. Therefore, it is very suitable for kinematic calibration of robots having multiple end-effectors. On the contrary, if we calibrate a robot having multiple end-effectors from its end-effectors to the base then at the link having two branching kinematic chains, we will need to estimate an additional transformation matrix for unifying the coordinate systems from different end-effectors [28].
4) The accuracy of our method depends upon two major factors, i.e., the calibration range and the radius of the 3-D circle (the distance between the calibration object and the rotation axis). For calibrating a prismatic joint, larger calibration range can make the calibration result more robust and accurate, because the 3-D line fitting will be more accurate when using a longer

linear trajectory of the calibration object. For calibrating a revolute joint, the calibration results obtained by our method can be more accurate when the calibration range and the radius of the trajectory are large enough. This is because when the calibration range approaches 360°, the circular trajectory of the calibration object tends to be a complete 3-D circle, and the 3-D circle fitting using data distributed in the complete circle will be more accurate than the one using only partial information of a circle. Also, larger radius will provide larger S/N ratio, and a very small radius will make the circular trajectory of the calibration object indistinguishable from the measurement noise.

We have performed the error analysis of several closed-form solutions for kinematic calibration (including the methods using pose measurements and the method using point measurements) and have described the results in [29]. From the error analysis results, we found that one limitation of the proposed method is that, when the calibration range of a revolute joint is very small (e.g., less than 40°), our method using only point measurements will become more sensitive to noise than with the methods using pose measurements. However, because we only have to measure the position of a single calibration point, the calibration object can be made very small. Therefore, when using stereo vision measurement systems, the calibration range can be easily made much larger. As the calibration range becomes larger, the calibration results will become much more accurate. The proposed closed-form solution has been applied to solve the kinematic calibration problem of a branched kinematic chain having two end-effectors. Notice that the complexity of implementing the proposed method is approximately equal to that of implementing existing closed-form solutions using pose measurements. The experiments on calibrating our binocular head have shown that based on the same set of measurement data, our method of using point measurements can achieve higher accuracy than that of using pose measurements.

Theoretically, there should exist a closed-form solution using both the position and orientation measurements to provide an optimal estimate of the kinematic parameters. However, existing closed-form solutions based on pose measurements only use the orientation information when estimating the orientation of the joint axes. Hence, the orientation error of the estimated kinematic model would be of the same order of the orientation measurement error. Furthermore, it is well known that to accurately estimate the orientation of a robot is a very difficult problem. Therefore, if no accurate pose estimation method is provided, we should not expect accurate kinematic calibration results when using the existing closed-form solutions based on pose measurements.

ACKNOWLEDGMENT

The authors would like to thank Dr. H. Zhuang and Dr. K.-Y. Young for their useful suggestions and discussions.

REFERENCES

[1] J. Aloimonos and A. Badyopadhyay, "Active vision," in *1st Int. Conf. Computer Vision*, 1987, pp. 35–54.

[2] R. Deriche, Z. Zhang, Q. T. Luong, and O. Faugeras, "Robust recovery of the epipolar geometry for and uncalibrated stereo rig," in *Lecture Notes Computer Science, Computer Vision—ECCV'94*, 1994, vol. 800, pp. 565–576.

[3] R. K. Krotkov, *Active Computer Vision by Cooperative Focus and Stereo*. New York: Springer-Verlag, 1989.

[4] A. L. Abbott, "Dynamic integration of depth cues for surface reconstruction from stereo images," Ph.D. dissertation, Univ. Illinois, Urbana-Champaign, 1990.

[5] D. J. Bennett and J. M. Hollerbach, "Identifying the kinematics of robots and their tasks," in *IEEE Int. Conf. Robotics Automation*, 1989, pp. 580–586.

[6] J. L. Caenen and J. C. Angue, "Identification of geometric and non geometric parameters of robots," in *IEEE Int. Conf. Robotics Automation*, 1990, pp. 1032–1037.

[7] G. Duelen, U. Kirchhoff, and J. Held, "Methods of identification of geometrical data in robot kinematics," *Robot. Comput. Integr. Manuf.*, vol. 4, no. 1/2, pp. 181–185, 1988.

[8] S. Hayati, K. Tso, and G. Roston, "Robot geometry calibration," in *IEEE Int. Conf. Robotics Automation*, 1988, pp. 947–951.

[9] W. Khalil, M. Gautier, and C. Enguehar, "Identifiable parameters and optimum configurations for robots calibration," *Robotica*, vol. 9, pp. 63–70, 1991.

[10] D. H. Kim, K. H. Cook, and J. H. Oh, "Identification and compensation of robot kinematic parameter for positioning accuracy improvement," *Robotica*, vol. 9, pp. 99–105, 1991.

[11] B. W. Mooring and T. J. Pack, "Calibration procedure for an industrial robot," in *IEEE Int. Conf. Robotics Automation*, 1988, pp. 786–791.

[12] W. K. Veitschegger and C. Wu, "A method for calibrating and compensating robot kinematic errors," in *IEEE Int. Conf. Robotics Automation*, 1987, pp. 39–44.

[13] X. L. Zhong and J. M. Lewis, "A new method for autonomous robot calibration," in *IEEE Int. Conf. Robotics Automation*, Nagoya, Japan, 1995, pp. 1790–1795.

[14] H. Zhuang, Z. S. Roth, and F. Hamano, "A complete and parametrically continuous kinematic model for robot manipulators," *IEEE Trans. Robot. Automat.*, vol. 8, no. 4, pp. 451–463, 1992.

[15] H. Zhuang and Z. S. Roth, "A linear solution to the kinematic parameter identification of robot manipulator," *IEEE Trans. Robot. Automat.*, vol. 9, no. 2, pp. 174–185, 1993.

[16] S. W. Shih, Y. P. Hung, and W. S. Lin, "Comments on 'a linear solution to kinematic parameter identification of robot manipulator' and some modifications," *IEEE Trans. Robot. Automat.*, vol. 11, no. 5, pp. 777–780, 1995.

[17] G. S. Young, T. H. Hong, M. Herman, and J. C. S. Yang, "Kinematic calibration of an active camera system," in *IEEE Proc. Int. Conf. Computer Vision Pattern Recognition*, 1992, pp. 748–751.

[18] R. K. Lenz and R. Y. Tsai, "Calibrating a Cartesian robot with eye-on-hand configuration independent of eye-to-hand relationship," *IEEE Trans. Pattern Anal. Machine Intell.*, vol. 11, no. 9, pp. 916–928, 1989.

[19] B. W. Mooring, Z. S. Roth, and M. R. Driels, *Fundamentals of Manipulator Calibration.* New York: Wiley, 1991.

[20] R. Y. Tsai and R. K. Lenz, "A new technique for fully autonomous and efficient 3-D robotics hand/eye calibration," *IEEE Trans. Robot. Automat.*, vol. 5, no. 3, pp. 345–358, 1989.

[21] S. W. Shih, Y. P. Hung, and W. S. Lin, "Head/eye calibration of a binocular head by use of single calibration point," in *IEEE Southw. Symp. Image Analysis Interpretation*, Dallas, TX, 1994, pp. 154–159.

[22] H. Zhuang and Z. S. Roth, "A note on 'a linear solution to the kinematic parameter identification of robot manipulators'," *IEEE Trans. Robot. Automat.*, vol. 11, p. 922, Dec. 1995.

[23] H. W. Stone, *Kinematic Modeling, Identification, and Control of Robotic Manipulators.* Norwell, MA: Kluwer, 1987.

[24] M. E. Sklar, "Metrology and calibration techniques for the performance enhancement of industrial robots," Ph.D. dissertation, Univ. Texas, Austin, 1988.

[25] S. W. Shih, Y. P. Hung, and W. S. Lin, "Kinematic parameter identification of an binocular head and its error analysis," Tech. Rep. TR-94-006, Inst, Inform, Sci., Academia Sinica, Nankang, Taipei, Taiwan, R.O.C, 1994.

[26] ——, "Kinematic parameter identification of a binocular head using stereo measurements of single calibration point," in *IEEE Int. Conf. Robotics Automation*, Nagoya, Japan, 1995, pp. 1796–1801.

[27] K. S. Arun, T. S. Huang, and S. D. Blostein, "Least-square fitting of two 3-D point sets," *IEEE Trans. Pattern Anal. Machine Intell.*, vol. 9, no. 5, pp. 698–700, 1987.

[28] S. W. Shih, J. S. Jin, K. H. Wei, and Y. P. Hung, "Kinematic calibration of a binocular head using stereo vision with the complete and parametrically continuous model," in *SPIE Proc., Intelligent Robots, Computer Vision XI*, 1992, vol. 1825, pp. 643–657.

[29] S. W. Shih, Y. P. Hung, and W. S. Lin, "Error analysis on closed-form solutions for kinematic calibration," Tech. Rep. TR-IIS-96-014, Inst. Inform. Sci., Academia Sinica (ftp://140.109.23.242/pub/TechRpt/TR-IIS-96-014.ps.gz), Nankang, Taipei, Taiwan, R.O.C., 1996.